Biosensors and Bioelectronics 65 (2015) 238–244

Contents lists available at ScienceDirect

Biosensors and Bioelectronics

journal homepage: www.elsevier.com/locate/bios

A graphene oxide based fluorescence resonance energy transfer (FRET) biosensor for ultrasensitive detection of botulinum neurotoxin A (BoNT/A) enzymatic activity

Jingyu Shi [a], Jiubiao Guo [b], Gongxun Bai [c], Chunyu Chan [a], Xuan Liu [d], Weiwei Ye [a], Jianhua Hao [c], Sheng Chen [b], Mo Yang [a,*]

[a] Interdisciplinary Division of Biomedical Engineering, The Hong Kong Polytechnic University, Hung Hom, Kowloon, Hong Kong, PR China
[b] Department of Applied Biology and Chemical Technology, The Hong Kong Polytechnic University, Hong Kong, PR China
[c] Department of Applied Physics, The Hong Kong Polytechnic University, Hong Kong, PR China
[d] Institute of Textiles & Clothing, The Hong Kong Polytechnic University, Hong Kong, PR China

ARTICLE INFO

Article history:
Received 7 August 2014
Received in revised form
17 October 2014
Accepted 20 October 2014
Available online 23 October 2014

Keywords:
Graphene oxide (GO)
Botulinum neurotoxins (BoNTs)
SNAP-25
Green fluorescence protein (GFP)
Optical detection

ABSTRACT

Botulinum neurotoxins (BoNTs) are among the most potent toxic bacterial proteins for humans, which make them potential agents for bioterrorism. Therefore, an ultrasensitive detection of BoNTs and their active states is in great need as field-deployable systems for anti-terrorism applications. We report the construction of a novel graphene oxide (GO)-peptide based fluorescence resonance energy transfer (FRET) biosensor for ultrasensitive detection of the BoNT serotype A light chain (BoNT-LcA) protease activity. A green fluorescence protein (GFP) modified SNAP-25 peptide substrate (SNAP-25-GFP) was optimally designed and synthesized with the centralized recognition/cleavage sites. This FRET platform was constructed by covalent immobilization of peptide substrate on GO with BSA passivation which have advantages of low non-specific adsorption and high stability in protein abundant solution. BoNT-LcA can specifically cleave SNAP-25-GFP substrate covalently immobilized on GO to release the fragment with GFP. Based on fluorescence signal recovery measurement, the target BoNT-LcA was detected sensitively and selectively with the linear detection range from 1 fg/mL to 1 pg/mL. The limit of detection (LOD) for BoNT-LcA is around 1 fg/mL.

1. Introduction

Botulinum toxin is a protein neurotoxin produced by the bacterium *Clostridium botulinum*, which is first discovered as a contaminant of poorly preserved ham in the last 19th century (Montecucco and Molgó, 2005). It is considered as the most potent toxic substance in the world and has the potential to be used as biological weapons (Lamanna, 1959). The toxicity caused by botulinum neurotoxins is called botulism, a serious and life-threatening paralytic illness. There are four serotypes (A,B,E,F) of botulinum neurotoxins associated with human illness, and among them BoNT serotype A (BoNT/A) is the most commonly involved in human illness (Arnon et al., 2001). BoNT/A consists of a light chain (LcA) and a heavy chain connected by a disulfide bond, acting as a responsible toxic unit and a facilitated transmission unit, respectively. On molecular level, neurotoxicity of BoNT/A results from the light chain's specific cleavage at the site between 197 and 198 of SNAP-25 peptide, which is one component of SNARE complex proteins (Pellizzari et al., 1999). Therefore, BoNT/A light chain (BoNT-LcA) is the most important target for BoNT toxin detection and a sensitive and reliable detection of BoNT-LcA protease activity is in an urgent need for early diagnosis and effective treatment.

In previous studies, mouse bioassay is the most commonly used method and considered to be the standard in laboratory detection for BoNTs activity with high sensitivity and reliability (Shapiro et al., 1998). Although mouse bioassay method owns the limit of detection of around 20 pg/mL for BoNT/A, it still suffers from a few drawbacks including being time-consuming (4–6 days), laborious and expensive (Cai et al., 2007). Then, several *in vitro* immunoassays have been developed, such as enzyme-linked immunosorbent assays (ELISA) (Sharma et al., 2006; Lindstrom and Korkeala, 2006; Stanker et al., 2008), immune-magnetic beads (Gessler et al., 2006; Rivera et al., 2006), immunoaffinity column (Gessler et al., 2007; Attrée et al., 2007), and immuno-sensors

* Corresponding author. Fax: +852 2334 2429. .
E-mail address: Mo.Yang@polyu.edu.hk (M. Yang).

http://dx.doi.org/10.1016/j.bios.2014.10.050
0956-5663/

(Sapsford et al., 2008; Ligler et al., 2007; Schmidt et al., 2001). Most immunoassays are based on the strategy of antibody-toxin binding, and usually equipped with a faster (4–9 h) and more sensitive (10 pg/mL) performance in contrast to mouse bioassay. However, immunological assays can not provide the activity information of botulinum toxin, which can only detect the presence of toxin rather than the activity state of the toxin. In order to solve this problem, BoNT activity assays, based on the toxins' ability to cleave specific SNARE proteins, have been developed *via* various detection approaches such as mass spectroscopy (Kalb et al., 2008), surface plasma resonance (Lévêque et al., 2013), and fluorimetric methods (Schmidt and Stafford, 2003). Among various activity assays, fluorescence resonance energy transfer (FRET) based methods are promising with the advantage of simplicity and direct response (Dong et al., 2004; Gilmore et al., 2011; Mangru et al., 2005; Sun et al., 2009). For FRET assays, the existence of toxin and its enzyme activity can be determined simultaneously by fluorescent signal transduction upon one-step addition of target toxin. However, the current FRET assays for BoNT enzymatic activity detection are based on organic fluorophores which suffer from relatively low quenching efficiency and poor sensitivity with LOD in the scale of ng/mL (Dong et al., 2004; Gilmore et al., 2011; Mangru et al., 2005; Sun et al., 2009). The fluorescence quenching efficiency of organic fluorophores is largely dependent on short-range distance while the cleavage activity of BoNT-LcA requires quite a long substrate sequence for cleavage on SNAP-25 peptide (Schmidt and Bostian, 1997). Moreover, the current FRET assays for BoNT enzymatic activity detection rely on single-donor *versus* single-acceptor configuration which has relatively low FRET transfer efficiency.

Graphene oxide (GO), a 2D atomically thin structure lattice with carboxyl groups exposed on the edges and hydroxyls and epoxies groups on the basal plane, has increasingly been used in FRET sensing platforms as multiple fluorophores' acceptors with large contact area and super quenching ability (Wang et al., 2011; Morales-Narvaez and Merkoci, 2012; Huang and Liu, 2012). Additionally, GO as an excellent quencher provides long-range resonance energy transfer over 300 Å (Swathi and Sebastian, 2008, 2009). Therefore, GO is a perfect quencher choice for long peptide substrate based FRET system to monitor BoNT/A protease activities. However, the usage of GO based FRET sensor for BoNT toxin enzymatic activity detection has not been explored. Green fluorescence protein (GFP), is a 27 KDa polypeptide, which can emit green light under blue light or UV light. Compared with organic fluorescent dyes, GFP can be conveniently attached to a host protein by genetic engineering to form a fusion protein without purification and chemical modification. Moreover, GFP proteins are generally not toxic to cells, which is especially suitable for *in vivo* FRET application in living organism such as monitoring protein–protein interaction and protease activity in cells and bacteria (Errampalli et al., 1999; Piston and Kremers, 2007).

In this study, a GO based FRET biosensor was developed for BoNT-LcA protease activity detection. The FRET platform was established *via* stable covalent immobilization between GFP conjugated peptide substrate (SNAP-25-GFP) and GO, with GFP and GO as energy donor–acceptor pair. The specific cleavage of SNAP-25 protein was then investigated based on the exposure of GO-peptide sensing platform to BoNT-LcA. Once GO-SNAP-25-GFP complex was cleaved by the target toxin, the fluorescence recovery signal was measured for detection of the target toxin. The passivation effect and stability of peptide-conjugated GO complex in protein abundant solution were also explored.

2. Materials and methods

2.1. Materials

GO was prepared from raw graphite flakes using a modified Hummers method (Krishnamoorthy et al., 2011). N-hydroxysulfosuccinimide (Sulfo-NHS) and 1-ethyl-3-(3-dimethyl-aminopropyl) carbodiimide hydrochloride (EDC) were purchased from Sigma-Aldrich (St. Louis, MO, USA). All of these chemicals were used as received without further purification. Skimmed milk and apple juice were purchased from local retailers.

2.2. Plasmid construction and peptide synthesis

BoNT-LcA and SNAP-25 were synthesized according to the previous study (Chen and Barbieri, 2011). Briefly, BoNT-LcA fragments were constructed by amplifying DNA encoding Lc/A (1–425) of *Clostridium botulinum* serotype A1 hall strain and subcloning into pET-15b. Plasmids for encoding Lc/A were transformed into *Escherichia coli* BL21(DE3) RIL (Stratagene). *E. coli* was then cultured for protein expression and His-LCs were then extracted from broken cells and purified. SNAP-25 with residues of 141 to 206 was constructed by amplifying DNA encoding region and subcloning into pGEX-2 T. Expression plasmids encoding SNAP-25 were transformed into *E. coli* TG1. *E. coli* TG1was then cultured for protein expression. Finally, SNAP-25 was extracted and purified according to the previous study (Ye et al., 2013). For peptide labeling, GFP was coupled to C terminus of SNAP-25 to form SNAP-25-GFP substrates.

2.3. Characterization

Fourier transform infrared spectrum (FT-IR) spectra of GO and GO-peptide conjugate ware collected with a PerkinElmer Spectrum 100 FT-IR spectrometer (PerkinElmer Inc., USA). Zeta potential of GO and GO-peptide conjugate was measured by a Zeta-Plus Zeta Potential Analyzer (Brokhaven Instruments Corp., USA). AFM experiment was performed with a multifunctional Scanning Probe Microscopy (Digital Instruments NanoScope IV). Powder X-ray diffraction (XRD) pattern of the as-prepared GO was recorded using a Rigaku smart lab 9 kW (Rigaku, Japan) with Cu Kα radiation ($\lambda = 1.5406$ Å). Raman spectra of GO were measured by a Horiba Jobin-Yvon Raman system (LabRam HR800) equipped with a 488 nm laser excitation source.

2.4. Conjugation of GO and peptide

GO-SNAP-25-GFP FRET sensing platform was realized by EDC/NHS assisted covalent bonding. GO solution with 5 mg/mL was sonicated for 30 min, and diluted into a series of concentrations by dissolving in DI water. Then, a solution with 5 mM Sulfo-NHS and 1 mM EDC were added into the suspension of GO sheets. After shaking on a vortex mixer for 2 min and a bath sonication for 15 min, a solution containing 0.12 μg/mL SNAP-25-GFP was added into the mixture. In order to achieve optimal quenching efficiency, the concentrations of GO were increased from 0 to 120 μg/mL, while the concentration of peptide was fixed at 0.12 μg/mL. The complex samples were sonicated in dark environment at room temperature for 1 h. The products were then purified by repeated centrifugation at 100,000 rpm for 30 min. The centrifugate was then rinsed with DI-water and resuspended in the solution of BSA 0.5 mg/mL for 30 min at room temperature. The product was centrifuged again at 100,000 rpm for 10 min and washed with DI water and resuspended in Tris buffer to obtain GO-SNAP-25-GFP complex.

2.5. Stability of peptide-conjugated GO complex

To prepare peptide-adsorbed GO complex, a simple self-assembly procedure was applied by incubation of SNAP-25-GFP peptide with GO. Firstly, GO (60 μg/mL, 40 μL) was mixed with SNAP-25-GFP peptide (0.12 μg/mL, 20 μL) and followed by incubation at room temperature for 2 h. The resulted complex was then purified by centrifugation and resuspended in Tris buffer. The peptide-conjugated GO complex was prepared based on the previously described conjugation procedures. BSA solution with concentration at 0.1 mg/mL was added into peptide-adsorbed GO complex and peptide-conjugated complex, respectively. The fluorescence intensity change with time was measured using a Tecan Infinite 200 microplate reader.

2.6. GO-peptide FRET effect and BoNT-LcA activity detection

Fluorescence spectra for FRET quenching efficiency and BoNT-LcA enzymatic activity assay were recorded using an Edinburgh FLSP920 spectrophotometer equipped with a 450 W steady-state xenon lamp at room temperature. The samples were collected in a 350 μL micro-scale quartz cuvette with excitation of 468 nm and emission of 510 nm. For FRET quenching experiments, GO with increasing concentrations was used to monitor the fluorescence signal change, which also reflected the influence of GO concentrations on quenching efficiency distinctly. The solution with GO-peptide conjugates was mixed with various concentrations of BoNT LcA toxin diluted (1 fg/mL, 10 fg/mL, 100 fg/mL, 1 pg/mL 10 pg/ mL) and incubated. All fluorescence spectra were collected under the same conditions.

3. Results

3.1. Mechanism of GO-peptide FRET biosensor

The sensing principle using GO-peptide based FRET biosensor for detection of enzymatic activity of BoNT-LcA is shown in Fig. 1. The protease substrate peptide used in this work is SNAP-25-GFP (residues from 141 to 206). In designing such a GO-based FRET biosensing platform, GO sheets are covalently conjugated with N terminus of SNAP-25-GFP by EDC/NHS activation, which brings GFP and GO into close proximity. Here, GFP and GO act as the energy transfer donor and energy transfer acceptor of FRET pair, respectively. In addition, bovine serum albumin (BSA) is used as the blocking agent to decrease the non-specific adsorption. Under 488 nm laser excitation, the emission of GFP is absorbed by GO. This GO-SNAP-25-GFP system is in a highly quenched state due to the ultra-high quenching efficiency of GO. In the presence of target BoNT-LcA, the SNAP-25-GFP substrate is cleaved into two fragments. As a result, the fragment with GFP is released from GO surface and the fluorescence signal is recovered. By measuring the recovered fluorescence signal, BoNT-LcA enzymatic activity can be monitored.

3.2. Characterization of synthesized GO

To realize the design, GO sheets were synthesized according to the previous research and the GO dispersion with particle size under 100 nm was obtained in water (Krishnamoorthy et al., 2011). The GO products were characterized by XRD spectra (Fig. 2a), which showed the characteristic peak of GO at $2\Theta = 10.58°$. Raman spectrum was also used to characterize GO products which had the well-documented strong peak at 1580 cm^{-1} (G band) and a weak peak at 1350 cm^{-1} (D band) (Fig. 2b). SNAP-25 was synthesized as a fusion protein coupled with GFP in the C terminus to form SNAP-25-GFP substrates. In the presence of N-hydroxysulfosuccinimide (Sulfo-NHS) and 1-ethyl-3-(3-dimethyl-aminopropyl) carbodiimide hydrochloride (EDC), SNAP-25-GFP substrates reacted with GO to form covalent amide bonding and brought into GO surface in close distance to facilitate FRET effect. The formation of GO-peptide complex was verified by AFM measurements. Fig. 2c shows the AFM images of bare GO in tapping mode to simultaneously collect image and height data. The AFM profile showed that the thickness of the synthesized GO sheets was around 1 nm (Fig. 2c). When GO was conjugated with SNAP-25-GFP, the heights of the complex were approximately around 8–10 nm, which indicated that SNAP-25-GFP was conjugated with GO surface (Fig. 2d).

3.3. Conjugation of GO and peptide

FTIR spectra were recorded to characterize the chemical structure of GO and GO-peptide conjugates as shown in Fig. S1 (in Supporting information). The characteristic peaks of GO were observed including peaks for O–H at 3401 cm^{-1}, C=O at

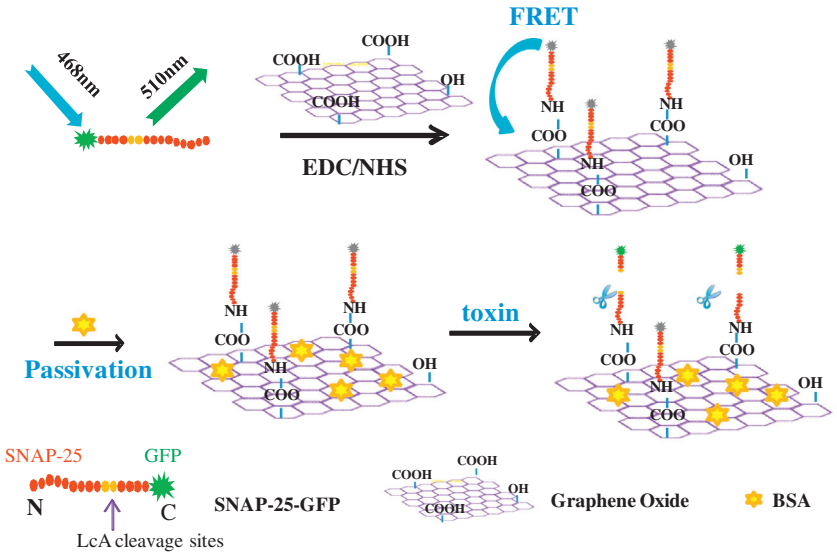

Fig. 1. Schematic diagram of BoNT-LcA enzymatic activity detection by the FRET biosensor based on energy transfer from GFP to GO.

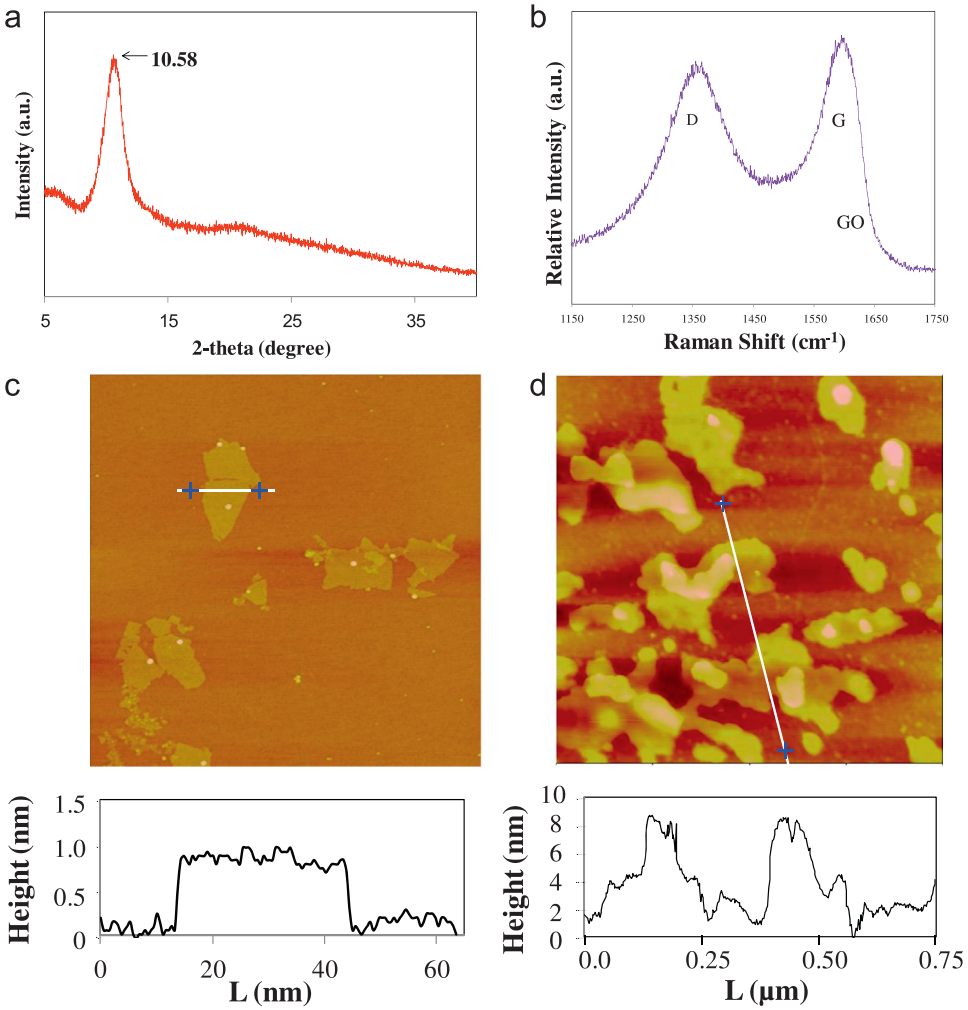

Fig. 2. (a) XRD spectrum of GO giving typical diffraction peak at 10.58°; (b) Raman spectrum of GO; AFM images and height profiles of (c) GO and (d) GO-SNAP-25-GFP complex.

1735 cm^{-1}, C=C at 1628 cm^{-1}, C–OH at 1384 cm^{-1}, and C–O at 1095 cm^{-1} respectively. For the GO-peptide complex, conjugation of SNAP-25-GFP peptide on GO was confirmed by the appearance of characteristic peaks corresponding to the $-CH_2-$ stretching vibration (2935 cm^{-1} and 2877 cm^{-1}), and amide group vibration (1647 cm^{-1} and 1553 cm^{-1}). Zeta potential measurements showed that GO-peptide was less negative charged compared with bare GO (Fig. S2, in Supporting information). The average zeta potential for bare GO was −40.7 mV at pH=7 due to plenty of negative charged oxygen groups on GO surface such as hydroxyl (–OH), carboxyl (COOH), epoxy (C–O–C), and caboxylate (COO–) which was similar to the previous reports (Konkena and Vasudevan, 2012). The average zeta potential shifted to −16.68 mV at pH=7 for GO-peptide complex after SNAP-25-GFP conjugation which was due to the less negative charged SNAP-25-GFP peptide immobilized on GO surface.

3.4. *Passivation effect and stability of peptide-conjugated GO complex*

To demonstrate the passivation effect of BSA on GO surface, adsorption experiments of SNAP-25-GFP peptide (0.12 μg/mL) on GO (60 μg/mL) without EDC/NHS treatment before and after BSA passivation were explored. As shown in Fig. 3a, bare GO without passivation caused a significant fluorescence intensity reduction of solution due to the adsorption of SNAP-25-GFP on GO surface. This adsorption brought SNAP-25-GFP peptide into proximity of GO and triggered FRET quenching effect with a high quenching ratio of 92.6% at wavelength of 510 nm. In contrast, negligible quenching effect was observed for bare GO after passivation with a low quenching ratio of 3.2%, which indicated that adsorption of peptide was negligible on GO after passivation. The results demonstrated that passivation on GO surface could significantly decrease non-specific peptide adsorption on GO. Using EDC/NHS chemical linkage method combined with passivation, most SNAP-25-GFP peptides attached to GO surface by covalent bonds rather than non-specific adsorption.

To compare the stability of peptide-conjugated GO complex and noncovalent peptide-adsorbed GO composite in complex matrix such as protein abundant solution, the fluorescence signal change was measured for both SNAP-25-GFP peptide adsorbed GO composite and SNAP-25-GFP peptide conjugated GO complex in BSA solution with the same concentration of 0.1 mg/mL. As shown in Fig. 3b, substantial enhancement of fluorescence signal was observed for peptide-adsorbed GO composite in BSA solution, which suggested the displacement of SNAP-25-GFP peptide from GO surface by BSA. In contrast, covalent conjugated GO-peptide complex only showed very slightly increased fluorescence signals, indicating the stability of covalent conjugated GO-peptide complex. This experiment demonstrated the weak affinity of peptide adsorbed on GO in the protein abundant solution. The results also showed that peptide-adsorbed GO complex based FRET biosensor

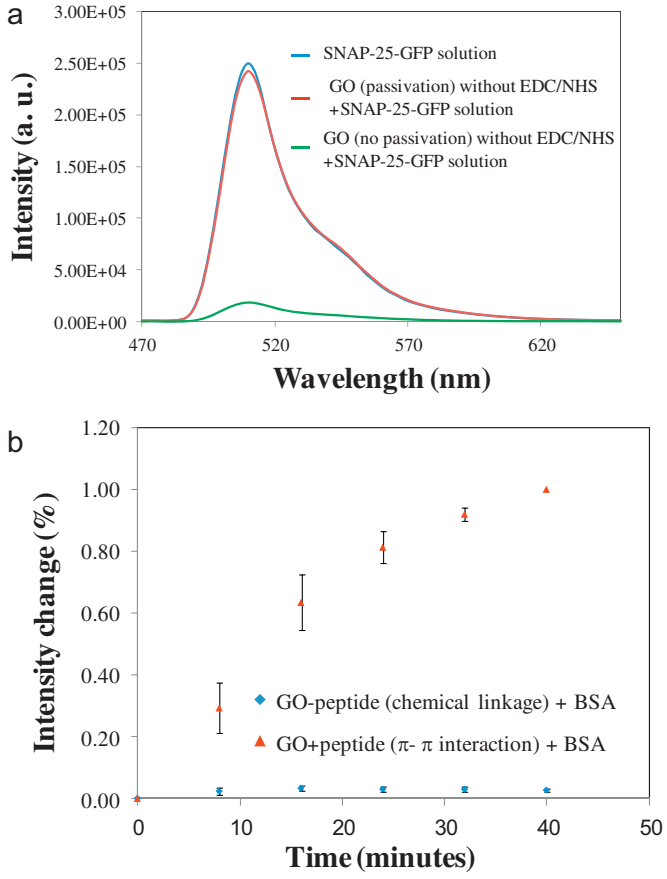

Fig. 3. (a) Fluorescence spectra of bare GO with and without passivation after addition of SNAP-25-GFP; (b) fluorescence signal change for peptide adsorbed GO composite and peptide conjugated GO complex in BSA solution with the same concentration of 0.1 mg/mL.

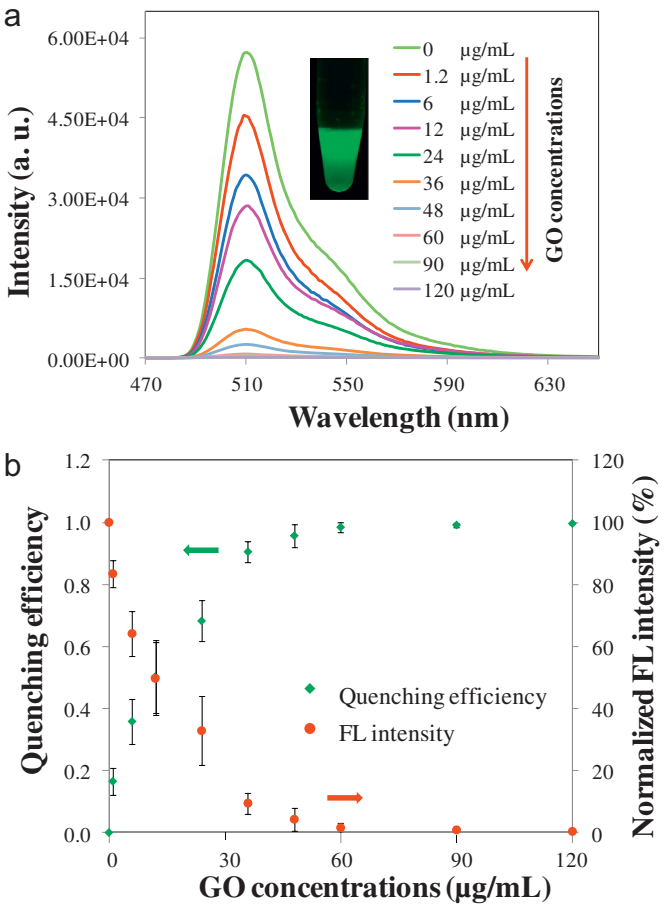

Fig. 4. (a) Fluorescence emission spectra of GO-SNAP-25-GFP complex in the presence of various GO/SNAP-25-GFP ratios; (b) quenching efficiency and normalized fluorescence intensity with various GO/SNAP-25-GFP ratios.

had low specificity in protein abundant solution, whose fluorescence signal recovery could be from non-specific protein replacement. Therefore, peptide-conjugated GO complex plus passivation is a better FRET-based peptide assay platform compared with peptide-adsorbed GO composite.

3.5. Construction of GO-peptide FRET biosensor

With 468 nm light illumination, SNAP-25-GFP solution emits intense green emission (inset of Fig. 4a). The green emission is attributed to the existence of the emission band centered at 510 nm. Energy transfer from GFP to GO was then explored by measuring the fluorescence quenching of GFP after addition of GO. Herein, a fixed 20 μL of SNAP-25-GFP with a concentration of 0.12 μg/mL was used. A 40 μL of GO solution with a series of concentrations was then added to SNAP-25-GFP solution for incubation and the fluorescence signals were then measured. The same volume of DI water was added to the SNAP-25-GFP solution and the related fluorescence signals were measured as control. Fig. 4a shows the fluorescence spectra of SNAP-25-GFP when GO were conjugated to form GO-SNAP-25-GFP complexes with increasing concentrations. Generally, upon mixing GO with SNAP-25-GFP, the fluorescence signals decreased gradually with increasing concentrations of GO from 0 μg/mL to 120 μg/mL. As a result of conjugation between GO and SNAP-25-GFP, SNAP-25-GFP was brought close to GO surface and fluorescence quenching was realized. The quenching efficiency is expressed by $Q=1-F_q/F_0$, where F_q is the fluorescence intensity of SNAP-25-GFP after quenching, and F_0 is the original fluorescence intensity of SNAP-25-GFP. As shown in Fig. 4b, the fluorescence quenching efficiency at 510 nm reached a maximum of 98% and the normalized fluorescence intensity (F_q/F_0) reached 1.6% when GO concentration increased to 60 μg/mL. The quenching efficiency kept almost unchanged when GO concentration further increased. This high quenching efficiency of 98% was due to the excellent quenching capability of GO.

3.6. Fluorescence signal recovery for LcA protease activity detection

Having demonstrated the quenching efficiency of GO on SNAP-25-GFP, we explored the use of GO-SNAP-25-GFP complex as the substrate for BoNT-LcA protease activity detection. GO-SNAP-25-GFP complex prepared with weight ratio of 60 μg/mL (GO) to 0.12 μg/mL (BoNT-LcA) was used for BoNT-LcA protease activity detection based upon the criteria of efficient FRET. This ratio could ensure the maximum quenching efficiency of 98% and the possible largest quenching efficiency change due to protease activity of BoNT-LcA. Exposing the GO-peptide FRET platform to a series of concentrations of BoNT-LcA for 30 min, fluorescence emission spectra were then measured to quantify the fluorescence recovery signals. Fig. 5a shows the fluorescence emission spectra of GO-SNAP-25-GFP complex with addition of a series of concentrations of BoNT-LcA from 1 fg/mL to 10 pg/mL. On mixing GO-SNAP-25-GFP complex with increasing concentrations of BoNT-LcA, the fluorescence signal was gradually recovered, as a result of the increasing cleavage action of BoNT-LcA to release the cleaved fragment with GFP from GO surface to the solution. Fig. 5b shows the relative fluorescence signal recovery rate $(F_r-F_q)/F_q$, where F_r is

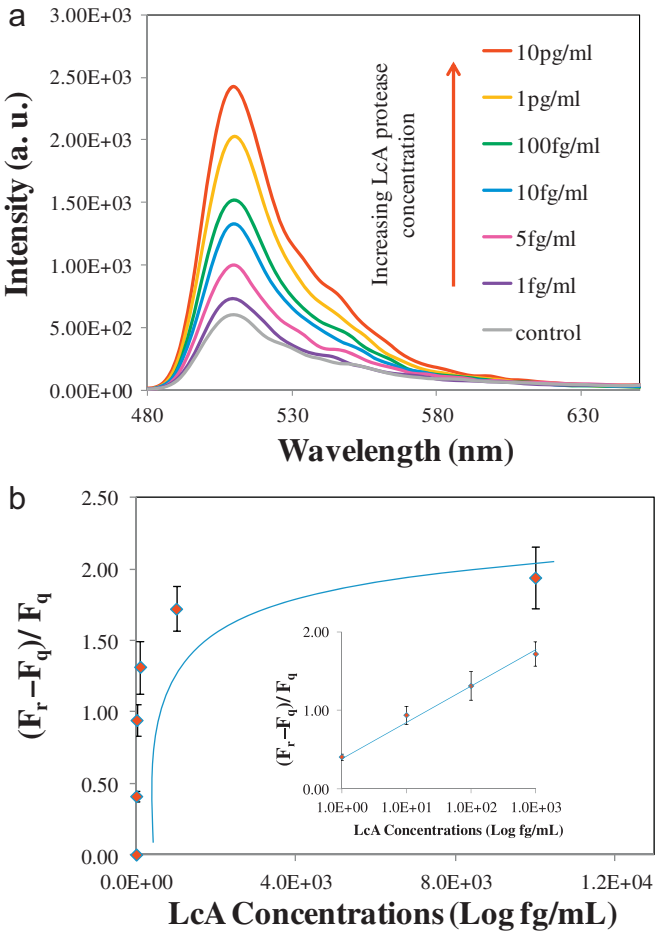

Fig. 5. (a) Fluorescence emission spectra of GO-SNAP-25-GFP complex with addition of BoNT-LcA with various concentrations from 1 fg/mL to 10 pg/mL. (b) Relative fluorescence intensity recovery $(F_r-F_q)/F_q$ for various concentrations from 1 fg/mL to 10 pg/mL. Inset: linear detection range from 1 fg/mL to 1 pg/mL.

the recovered fluorescence intensity of SNAP-25-GFP after addition of BoNT-LcA, and F_q is the fluorescence intensity of SNAP-25-GFP after quenching. As shown in Fig. 5b, this FRET biosensor shows a quantifiable detection range from 1 fg/mL to 10 pg/mL and a linear detection range from 1 fg/mL to 1 pg/mL (inset of Fig. 5b). The limit of detection (LOD) for BoNT-LcA protease activity detection is around 1 fg/mL based on the background signal plus 3 times of standard derivation. These results are superior to the current detection methods including mouse bioassay (Shapiro et al., 1998), immunoassays (Cai et al., 2007; Lindstrom and Korkeala, 2006; Sapsford et al., 2008), organic fluorophore based FRET biosensors and the commercial available FRET kits (Dong et al., 2004; Gilmore et al., 2011; Mangru et al., 2005; Sun et al., 2009; Feltrup and Singh, 2012), whose BoNT LODs are in the range from 1 pg/mL to 1 ng/mL.

3.7. Performance evaluation of FRET biosensor

The specificity of this FRET biosensor to BoNT-LcA toxin was explored in control experiments with BoNT serotype B light chain (BoNT-LcB) which was tested with identical procedures with BoNT-LcA. BoNT/B is also toxic to humans but does not cleave SNAP-25 substrate. Instead, BoNT/B specifically cleaves another substrate of neuronal vesicle-associated membrane protein (VAMP) (Frisk et al., 2011). With the same concentration (0.7 mg/mL), BoNT-LcB did not cause an obvious recovery of donor fluorescence signals while BoNT-LcA could lead to a large increase

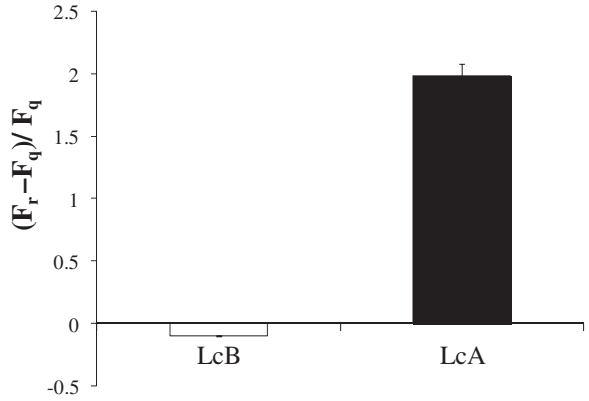

Fig. 6. Comparison of fluorescence signal recovery between target BoNT-LcA and non-target BoNT-LcB.

of fluorescence signals. It demonstrated that this FRET biosensor was specific for BoNT-LcA and insensitive to BoNT-LcB (Fig. 6).

The repeatability of the proposed GO-peptide FRET biosensor was investigated by evaluating the variation of experimental results for 10 proposed GO-peptide FRET biosensor. The standard deviation was 7.9% at 0.1 pg/mL LcA concentration in Tris buffer solution. The results indicated that the proposed GO-peptide FRET biosensor was robust for LcA detection with acceptable repeatability.

To evaluate the ability of this FRET biosensor for practical applications, LcA protease activity detection was explored in skimmed milk and apple juice. BoNT-LcA toxin at 0.1 pg/mL was spiked into skimmed milk and apple juice, respectively. Fluorescence recovery signal measured in Tris buffer solution was used as the reference for comparison. The experimental conditions were the same with previous experiments. As shown in Fig. S3 (in Supporting information), there was no observable fluorescence recovery rate difference between toxin-spiked buffer and toxin-spiked apple juice, indicating apple juice has no significant effect on performance of this FRET biosensor for LcA toxin detection. In toxin-spiked skimmed milk, the fluorescence recovery rate was decreased to around 52% of that in buffer, but still obviously larger than that of non-spiked sample. The decrease of fluorescence recovery signal could be explained by the interference from abundant amount of protein in skimmed milk. The above results demonstrated the potential applicability of this FRET biosensor for real food sample detection.

4. Conclusion

In summary, we have constructed a novel GO-peptide FRET based proteolytic biosensor for bacteria protein toxin BoNT-LcA detection. The ability of long-range energy transfer and high quenching efficiency of GO allows the assembly of lengthy peptide substrate sequence on GO surface for the access of LcA toxin. Moreover, the large planar surface area of GO provides the simultaneous quenching capability which is unavailable to conventional FRET based BoNT enzymatic activity assay with a single-donor *versus* single-acceptor dye configuration. This peptide-conjugated GO complex based FRET system with BSA passivation could decrease non-specific adsorption and keep high stability in protein abundant solution compared with peptide-adsorbed GO composite. The LOD of 1 fg/mL for BoNT-LcA using this GO-peptide FRET biosensor is much lower than current dominating methods including mouse bioassay, immunoassays and the commercial available FRET kits, whose LOD is around 1 pg/mL to 1 ng/mL. This GO-peptide FRET biosensor can be easily adapted to the detection

of other BoNT serotypes with alternative peptide substrates, which provides an ultrasensitive platform as BoNT enzymatic activity assay. Therefore, peptide-conjugated GO complex plus passivation is a better FRET-based peptide assay platform compared with peptide-adsorbed GO composite.

Acknowledgment

This research was supported partially by the Hong Kong Research Council General Research Grant (PolyU5305/11E) and partially supported by the internal research grant of the Hong Kong Polytechnic University (G-YN03).

Appendix A. Supplementary material

Supplementary data associated with this article can be found in the online version at http://dx.doi.org/10.1016/j.bios.2014.10.050.

References

Attrée, O., Guglielmo-Viret, V., Gros, V., Thullier, P., 2007. J. Immunol. Methods 325, 78–87.
Arnon, S.S., Schechter, R., Inglesby, T.V., Henderson, D.A., Bartlett, J.G., Ascher, M.S., Eitzen, E., Fine, A.D., Hauer, J., Layton, M., Lillibridge, S., Osterholm, M.T., O'Toole, T., Parker, G., Perl, T.M., Russell, P.K., Swerdlow, D.L., Tonat, K., 2001. JAMA: J. Am. Med. Assoc. 285, 1059–1070.
Chen, S., Barbieri, J.T., 2011. J. Biol. Chem. 286, 15067–15072.
Cai, S.W., Singh, B.R., Sharma, S., 2007. Crit. Rev. Microbiol. 33, 109–125.
Dong, M., Tepp, W.H., Johnson, E.A., Chapman, E.R., 2004. Proc. Natl. Acad. Sci. USA 101, 14701–14706.
Errampalli, D., Leung, K., Cassidy, M.B., Kostrzynska, M., Blears, M., Lee, H., Trevors, J. T., 1999. J. Microbiol. Methods 35, 187–199.
Frisk, M.L., Lin, G., Johnson, E.A., Beebe, D.J., 2011. Biosens. Bioelectron. 15, 1929–1935.
Feltrup, T.M., Singh, B.R., 2012. Anal. Chem. 84, 10549–10553.
Gessler, F., Hampe, K., Schmidt, M., Böhnel, H., 2006. Diagn. Microbiol. Infect. Dis. 56, 225–232.
Gessler, F., Pagel-Wieder, S., Avondet, M.A., Böhnel, H., 2007. Diagn. Microbiol. Infect. Dis. 57, 243–249.
Gilmore, M.A., Williams, D., Okawa, Y., Holguin, B., James, N.G., Ross, J.A., Roger Aoki, K., Jameson, D.M., Steward, L.E., 2011. Anal. Biochem. 413, 36–42.
Huang, P.-J.J., Liu, J., 2012. Small 8, 977,, 977.
Konkena, B., Vasudevan, S., 2012. J. Phys. Chem. Lett. 3, 867–872.
Krishnamoorthy, K., Mohan, R., Kim, S.J., 2011. Appl. Phys. Lett. 98, 244101.
Kalb, S.R., Smith, T.J., Moura, H., Hill, K., Lou, J.L., Geren, I.N., Garcia-Rodriguez, C., Marks, J.D., Smith, L.A., Pirkle, J.L., Barr, J.R., 2008. Int. J. Mass Spectrom. 278, 101–108.
Lamanna, C., 1959. Science 130, 763–772.
Lévêque, C., Ferracci, G., Maulet, Y., Grand-Masson, C., Blanchard, M.P., Seagar, M., El Far, O., 2013. Biosens. Bioelectron. 49, 276–281.
Ligler, F.S., Sapsford, K.E., Golden, J.P., Shriver-Lake, L.C., Taitt, C.R., Dyer, M.A., Barone, S., Myatt, C.J., 2007. Anal. Sci. 23, 5–10.
Lindstrom, M., Korkeala, H., 2006. Clin. Microbiol. Rev. 19, 298–314.
Montecucco, C., Molgó, J., 2005. Curr. Opin. Pharmacol. 5, 274–279.
Morales-Narvaez, E., Merkoci, A., 2012. Adv. Mater. 24, 3298–3308.
Mangru, S., Bentz, B.L., Davis, T.J., Desai, N., Stabile, P.J., Schmidt, J.J., Millard, C.B., Bavari, S., Kodukula, K., 2005. J. Biomol. Screen., 10; , pp. 788–794.
Pellizzari, R., Rossetto, O., Schiavo, G., Montecucco, C., 1999. Philos. Trans.: Biol. Sci. 354, 259–268.
Piston, D.W., Kremers, G.J., 2007. Trends Biochem. Sci. 32, 407–414.
Rivera, V.R., Gamez, F.J., Keener, W.K., White, J.A., Poli, M.A., 2006. Anal. Biochem. 353, 248–256.
Stanker, L.H., Merrill, P., Scotcher, M.C., Cheng, L.W., 2008. J. Immunol. Methods 336, 1–8.
Schmidt, J.J., Bostian, K.A., 1997. J. Protein Chem. 16, 19–26.
Schmidt, J.J., Stafford, R.G., Millard, C.B., 2001. Anal. Biochem. 296, 130–137.
Schmidt, J.J., Stafford, R.G., 2003. Appl. Environ. Microbiol. 69, 297–303.
Sapsford, K.E., Sun, S., Francis, J., Sharma, S., Kostov, Y., Rasooly, A.A., 2008. Biosens. Bioelectron. 24, 618–625.
Sun, S., Ossandon, M., Kostov, Y., Rasooly, A., 2009. Lab Chip 9, 3275–3281.
Swathi, R.S., Sebastian, K.L., 2009. J. Chem. Phys. 130, 086101.
Swathi, R.S., Sebastian, K.L., 2008. J. Chem. Phys. 129, 054703.
Shapiro, R.L., Hatheway, C., Swerdlow, D.L., 1998. Ann. Intern. Med. 129, 221–228.
Sharma, S.K., Ferreira, J.L., Eblen, B.S., Whiting, R.C., 2006. Appl. Environ. Microbiol.. 72, 1231–1238.
Wang, Y., Li, Z., Wang, J., Li, J., Lin, Y., 2011. Trends Biotechnol. 29, 205–212.
Ye, W.W., Guo, J.B., Chen, S., Yang, M., 2013. J. Mater. Chem. B 1, 6544–6550.